Constructing a variational ground state of matter fermions coupled to a vison pair in Kitaev's honeycomb model

Theo Grace [*] and Alessandro Principi [†]
Department of Physics and Astronomy, University of Manchester, Manchester M13 9PL, United Kingdom

(Received 2 December 2025; accepted 18 February 2026; published 11 March 2026)

We develop a method to construct simple and explicit variational approximations for the ground state of Kitaev's honeycomb model with a nontrivial $\mathbb{Z}_2$ flux configuration consisting of a pair of visons on neighboring plaquettes. The method consists of retaining only the largest singular values of the generator of the transformation between the vison pair and flux-free ground states. We compare physical quantities calculated using the approximate state to those obtained by extrapolating the results of exact diagonalization of finite lattices, finding them to be in very good agreement. We discuss ways to extend the method to more complicated flux configurations.

DOI: 10.1103/t64v-ch2p

I. INTRODUCTION

Kitaev's honeycomb model [1] is a much-studied exactly solvable model of a frustrated quantum magnet that realizes a quantum spin liquid (QSL). It exhibits the characteristic features of a QSL, with long-range entanglement of the ground state and fractionalized excitations [2,3]. In Kitaev's model the spins fractionalize into Majorana fermions interacting with an emergent $\mathbb{Z}_2$ gauge field, which gives rise to both gapless fermionic excitations (spinons) and gapped excitations due to π fluxes of the $\mathbb{Z}_2$ gauge field (visons).

The appeal of Kitaev's model is not solely for theoretical study of exotic phenomena. There are a growing number of materials for which Kitaev interactions are thought to be dominant [4,5], notably α-$RuCl_3$ [6,7]. However, despite evidence of strong Kitaev interactions, these materials are also found to magnetically order at low temperatures [8–10]. This has motivated extensive theoretical study of the interplay between the Kitaev Hamiltonian and other interactions expected in real materials, the largest of which are Heisenberg and symmetric off-diagonal (Gamma) interactions [11]. The inclusion of other terms in the Hamiltonian spoils its exact solution and produces a rich phase diagram with an extended Kitaev QSL phase as well as a number of competing conventionally ordered phases. This has been established through multiple techniques including parton mean-field theories [11,12], Monte Carlo methods [13], coupled chain analysis [14], and exact diagonalization [15].

An open area of research is finding signatures that can distinguish the QSL from competing phases in experiments. A means of detecting the emergent gauge field would be a valuable indicator of QSL behavior. Several recent theoretical works with this aim have focused on the dynamics of vison excitations in weakly perturbed Kitaev models [16–20]. The visons, which are static at the exactly solvable point [1], become mobile when other interactions are present. The motion of visons sets bounds on the stability of the spin liquid phase, which are dependent on the sign of the Kitaev coupling [19]. In magnetic fields visons may form topologically nontrivial bands for antiferromagnetic Kitaev coupling and contribute to a quantized thermal Hall effect [18,19]. The important role of $\mathbb{Z}_2$ fluxes in phases at higher magnetic field strengths is an active area of research, with recent work suggesting $\mathbb{Z}_2$ flux dynamics produces an emergent glassy phase [21] at intermediate field strengths. In weakly perturbed models pairs of visons on neighboring plaquettes can form bound states with spinons when Heisenberg and Gamma interactions are considered, which can destabilize the spin liquid for sufficiently strong interaction, and has a distinct signature in the spin structure factor [16]. The method developed in Ref. [16] relates hopping parameters for vison pairs, generalized to individual visons in [18,19], to matrix elements between exact eigenstates of the unperturbed Kitaev model with a fixed gauge. These can then be calculated numerically using exact diagonalization on finite lattices and extrapolated to infinite ones.

In order to develop an understanding of vison excitations beyond numerical work it is useful to find simple approximate explicit expressions for Kitaev eigenstates in the presence of vison excitations. The strong interaction between visons and spinons affects many vison properties, such as their excitation energy and mobility in perturbed Kitaev models, which in turn affects the stability of the spin liquid phase itself. In this work we calculate an approximate explicit expression for the lowest energy eigenstate of the Kitaev model with a nontrivial $\mathbb{Z}_2$ gauge field consisting of a pair of visons on neighboring

[*]Contact author: theo.grace@manchester.ac.uk
[†]Contact author: alessandro.principi@manchester.ac.uk

Published by the American Physical Society under the terms of the Creative Commons Attribution 4.0 International license. Further distribution of this work must maintain attribution to the author(s) and the published article's title, journal citation, and DOI.

TABLE I. Comparison of vison pair hopping amplitudes calculated using exact diagonalization on finite lattices extrapolated to infinite size and the variational approximation.

Interaction	Kitaev sign	Exact	Approximate
Heisenberg	FM	$0.0938J$[a]	$0.0991J$
	AFM	$1.4702J$[a]	$1.4964J$
Gamma	FM	-1.4391Γ[a]	-1.4632Γ
	AFM	-0.1733Γ[a]	-0.1809Γ
Zeeman	FM	$1.35ih$[b]	$1.387ih$
	AFM	$0.0494ih$[b]	$0.0495ih$

[a]Taken from [16].
[b]Taken from [17].

plaquettes. We show that a simple ansatz may be used to approximate the vison pair state, which we then optimize by minimizing the matter sector ground state energy. We then compare the results for hopping parameters of vison pairs obtained with our approximate method to those of Ref. [16] based on exact diagonalization. Our results are summarized in Table I. We note that the largest relative error is of the order of just ≈6%, which shows the good performance of the method we have developed. We stress that, compared to exact diagonalization for which the largest systems studied are of the order 100×100 unit cells, our method allows direct study of much larger lattices exceeding 1000×1000 unit cells.

The structure of the paper is as follows. In Sec. II we review Kitaev's honeycomb model and its exact solution. In Sec. III we provide a justification for the variational ansatz and for the application of the variational method to the determination of approximate eigenstates. In Sec. IV we compare the results from our approximation with those obtained via exact diagonalization. Finally, in Sec. V we discuss our results and draw conclusions, highlighting possible further applications of our method.

II. REVIEW OF KITAEV'S HONEYCOMB MODEL

Kitaev's honeycomb model describes spins $S = 1/2$ on a honeycomb lattice with a bond direction dependent Ising interaction between nearest neighbor spins [1]. The Hamiltonian is given by

$$\mathcal{H} = -K \sum_{\boldsymbol{r},\alpha} \sigma^{\alpha}_{\boldsymbol{r}} \sigma^{\alpha}_{\boldsymbol{r}+\boldsymbol{r}_\alpha}, \tag{1}$$

where σ^{α} ($\alpha = x, y, z$) are Pauli matrices, $\boldsymbol{r}$ labels a site on the A sublattice, while $\boldsymbol{r}_\alpha$ are the vectors connecting such site to its three nearest neighbors (which belong to the B sublattice). See Fig. 1 for the definition of $\boldsymbol{r}_\alpha$.

This Hamiltonian has an extensive number of conserved quantities that are crucial for its exact solution [1]. For each plaquette one can define a (conserved) "flux" operator as the product of Pauli matrices associated to exterior bonds [1] [see also Eq. (4) below]. The model can be exactly solved using Kitaev's representation of each spin in terms of four Majorana fermions, named $b^x_{\boldsymbol{r}}$, $b^y_{\boldsymbol{r}}$, $b^z_{\boldsymbol{r}}$, and $c_{\boldsymbol{r}}$, such that $\sigma^{\alpha}_{\boldsymbol{r}} = ib^{\alpha}_{\boldsymbol{r}} c_{\boldsymbol{r}}$. We will take the convention that the Majorana operators satisfy $\{c_{\boldsymbol{r}}, c_{\boldsymbol{r}'}\} = 2\delta_{\boldsymbol{r},\boldsymbol{r}'}$, $\{b^{\alpha}_{\boldsymbol{r}}, b^{\beta}_{\boldsymbol{r}'}\} = 2\delta_{\boldsymbol{r},\boldsymbol{r}'}\delta_{\alpha,\beta}$, and $\{c_{\boldsymbol{r}}, b^{\alpha}_{\boldsymbol{r}}\} = 0$.

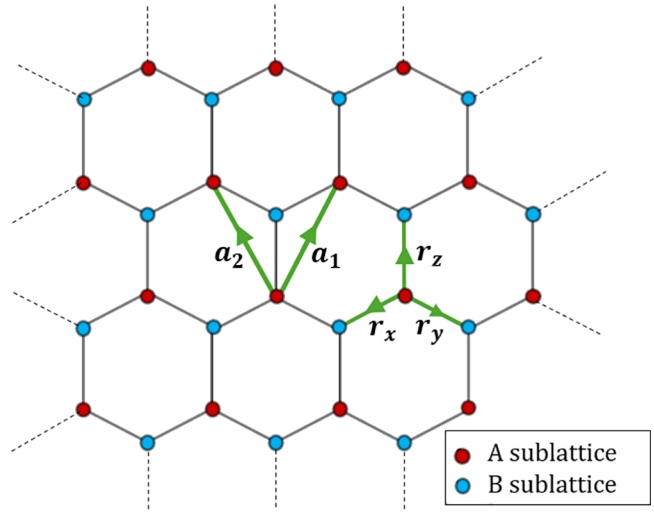


FIG. 1. The geometry of Kitaev's honeycomb model. $\mathbf{a}_1 = \frac{1}{2}(1, \sqrt{3})$ and $\mathbf{a}_2 = \frac{1}{2}(-1, \sqrt{3})$ are the primitive lattice vectors, while $\boldsymbol{r}_\alpha$ ($\alpha = x, y, z$) denotes the vectors connecting a site of sublattice A to its three B-type nearest neighbors. Dimensionless units are used such that $|\mathbf{a}_1| = |\mathbf{a}_2| = 1$.

Complex fermions formed from combinations of Majoranas denoted as $c_{\boldsymbol{r}}$ will be referred to as "matter" fermions. The Majorana representation has a larger Hilbert space than that of the spin states: only states that satisfy $D_{\boldsymbol{r}}|\psi\rangle = |\psi\rangle$ with $D_{\boldsymbol{r}} = b^x_{\boldsymbol{r}} b^y_{\boldsymbol{r}} b^z_{\boldsymbol{r}} c_{\boldsymbol{r}}$ represent physical spin states. The states in the enlarged Hilbert space can be projected onto the physical subspace by using the projection operator:

$$\hat{P} = \prod_{\boldsymbol{r}} \frac{1 + D_{\boldsymbol{r}}}{2}. \tag{2}$$

The Hamiltonian in the Majorana representation is given by

$$\mathcal{H}^{\hat{u}} = iK \sum_{\boldsymbol{r}\in A,\alpha} c_{\boldsymbol{r}} \hat{u}^{\alpha}_{\boldsymbol{r}} c_{\boldsymbol{r}+\boldsymbol{r}_\alpha}, \tag{3}$$

where $\hat{u}^{\alpha}_{\boldsymbol{r}} = ib^{\alpha}_{\boldsymbol{r}} b^{\alpha}_{\boldsymbol{r}+\boldsymbol{r}_\alpha}$ is a (conserved) link operator with eigenvalues ± 1. The link operators satisfy $[\hat{u}^{\alpha}_{\boldsymbol{r}}, \hat{u}^{\beta}_{\boldsymbol{r}'}] = 0$ and $[\hat{u}^{\alpha}_{\boldsymbol{r}}, \mathcal{H}^{\hat{u}}] = 0$, so the eigenstates may be labeled by their link operator eigenvalues. This allows eigenstates in the extended Hilbert space to be written as a tensor product of the state of the link variables denoted as $|u\rangle$ and the state of the matter fermions. The Hamiltonian is invariant under local $\mathbb{Z}_2$ transformations in which $c_{\boldsymbol{r}} \to (-1)^{n_{\boldsymbol{r}}} c_{\boldsymbol{r}}$, $\hat{u}^{\alpha}_{\boldsymbol{r}} \to (-1)^{n_{\boldsymbol{r}}} \hat{u}^{\alpha}_{\boldsymbol{r}} (-1)^{n_{\boldsymbol{r}+\boldsymbol{r}_\alpha}}$ with site dependent $n_{\boldsymbol{r}} \in \{0, 1\}$. A Wilson loop given by a product of link operators $\hat{u}^{\alpha}_{\boldsymbol{r}}$ around a closed loop is invariant under a $\mathbb{Z}_2$ gauge transformation, and corresponds to the flux of the emergent $\mathbb{Z}_2$ gauge field through the loop. The smallest Wilson loop is around a single hexagonal plaquette:

$$W_p = \prod_{u^{\alpha}\in\partial p} \hat{u}^{\alpha}_{\boldsymbol{r}}. \tag{4}$$

The loop operators commute with the Hamiltonian and satisfy $[W_p, D_{\boldsymbol{r}}] = 0$ so physical states may be labeled by their $\mathbb{Z}_2$ flux configuration.

Acting on an eigenstate of the link operators $|u\rangle$ gives a Hamiltonian for the matter fermions that is quadratic in matter

fermion operators.

$$\mathcal{H}^u = iK \sum_{\boldsymbol{r},\boldsymbol{r}' \in A} c^A_{\boldsymbol{r}} M^u_{\boldsymbol{r},\boldsymbol{r}'} c^B_{\boldsymbol{r}'}. \tag{5}$$

Here $M^u_{\boldsymbol{r},\boldsymbol{r}'} = u^z_{\boldsymbol{r}}\delta_{\boldsymbol{r},\boldsymbol{r}'} + u^x_{\boldsymbol{r}}\delta_{\boldsymbol{r}-\mathbf{a}_1,\boldsymbol{r}'} + u^y_{\boldsymbol{r}}\delta_{\boldsymbol{r}-\mathbf{a}_2,\boldsymbol{r}'}$ is a link variable dependent matrix and the Majorana operators have been given explicit sublattice labels $c^A_{\boldsymbol{r}} = c_{\boldsymbol{r}}$ and $c^B_{\boldsymbol{r}} = c_{\boldsymbol{r}+\boldsymbol{r}_z}$. This may be diagonalized exactly by taking the singular value decomposition $M^u = U^u E^u V^{uT}$, where U^u and V^u are real orthogonal matrices and E^u is a diagonal matrix of singular values. The superscript u is used to highlight the dependence on the configuration (i.e., the eigenstates) of the link operators. Note that although the singular values E^u_k depend on the link configuration, they are independent of $\mathbb{Z}_2$ gauge transformations, so they only depend on the $\mathbb{Z}_2$ flux configuration. Using the singular value decomposition, one can rewrite the Hamiltonian:

$$\begin{aligned}\mathcal{H}^u &= iK \sum_k E^u_k C^{u,A}_k C^{u,B}_k \\ &= |K| \sum_k E^u_k \left(2\eta^{u\dagger}_k \eta^u_k - 1\right),\end{aligned} \tag{6}$$

where $C^{u,A}_k = U^{u,T}_{k,\boldsymbol{r}} c^A_{\boldsymbol{r}}$ and $C^{u,B}_k = V^{u,T}_{k,\boldsymbol{r}} c^B_{\boldsymbol{r}}$ are Majorana fermions that may be combined into a complex fermion that diagonalizes the matter sector Hamiltonian for a particular link variable configuration.

$$\eta^u_k = \left(C^{u,A}_k + iK/|K| C^{u,B}_k\right)/2. \tag{7}$$

Note that we have included a factor that depends on the sign of the Kitaev coupling in the definition of η^u_k to ensure η^u_k is an annihilation operator for both ferromagnetic and antiferromagnetic Kitaev interactions. The matter fermion ground state corresponding to a particular link variable configuration is then defined by

$$\eta^u_k |0^u\rangle = 0 \quad \forall k.$$

Lieb's Theorem [22] guarantees that the ground state of the model is in the fluxless sector in which the Wilson loop operator has eigenvalues $W_p = +1$ on all plaquettes. The simplest link configuration in this sector is the trivial configuration, labeled by u_0, in which all link variables are $u^\alpha_{\boldsymbol{r}} = +1$. For this configuration the corresponding matter sector Hamiltonian is a translationally invariant nearest neighbor hopping model, so the diagonalizing matter fermion operators may be found explicitly using a Fourier transformation [1].

$$\eta^{u_0}_{\boldsymbol{k}} = \frac{1}{\sqrt{2N}} \sum_{\boldsymbol{r}} \left(e^{i\boldsymbol{k}\cdot\boldsymbol{r}} c^A_{\boldsymbol{r}} + i\frac{K}{|K|} e^{i(\boldsymbol{k}\cdot\boldsymbol{r}+\varphi_{\boldsymbol{k}})} c^B_{\boldsymbol{r}} \right), \tag{8}$$

where $\varphi_{\boldsymbol{k}}$ is defined by $e^{i\varphi_{\boldsymbol{k}}} = \Delta_{\boldsymbol{k}}/|\Delta_{\boldsymbol{k}}|$ with $\Delta_{\boldsymbol{k}} = 1 + e^{i\boldsymbol{k}\cdot\mathbf{a}_1} + e^{i\boldsymbol{k}\cdot\mathbf{a}_2}$. The corresponding energies are $E^{u_0}_{\boldsymbol{k}} = 2|K||\Delta_{\boldsymbol{k}}|$. Note that the operators in Eq. (8) are not written as the sum of a Majorana operator on each sublattice in the form of Eq. (7). The operators $\eta^{u_0\dagger}_{\boldsymbol{k}}$ and $\eta^{u_0\dagger}_{-\boldsymbol{k}}$ create degenerate excitations, so may be combined into new eigenstate creation operators $\eta^{u_0}_{\boldsymbol{k},+} = (\eta^{u_0}_{\boldsymbol{k}} + \eta^{u_0}_{-\boldsymbol{k}})/\sqrt{2}$ and $\eta_{\boldsymbol{k},-} = i(\eta^{u_0}_{-\boldsymbol{k}} - \eta^{u_0}_{\boldsymbol{k}})/\sqrt{2}$ which do have the form of Eq. (7). The physical ground state is given by

$$|\Omega\rangle = \hat{P}(|u_0\rangle \otimes |0^{u_0}\rangle). \tag{9}$$

As well as the matter fermion excitations, there are excitations associated with link variable configurations in which there are Wilson loops with $W_p = -1$ on some of the plaquettes. These excitations, due to a flux of the emergent $\mathbb{Z}_2$ gauge field, are called visons.

III. MATTER FERMION GROUND STATE IN THE PRESENCE OF A VISON PAIR

A $\mathbb{Z}_2$ flux configuration with a pair of visons on neighboring plaquettes may be represented by a single link variable $u^\alpha_{\boldsymbol{r}} = -1$ with all others equal to $+1$. The position of a vison pair can be labeled by the link joining the plaquettes, which can be identified by a site $\boldsymbol{r}$ on the A sublattice and the link orientation α. For a vison pair at the origin separated by a z-oriented link, the link state may be written as $b^z_0 |u_0\rangle$ and the corresponding Hamiltonian for the matter fermions is $\mathcal{H}^{0,z}$, with ground state $|0^{0,z}\rangle$. The Hamiltonian $\mathcal{H}^{0,z}$ can be written as the sum of the trivial link configuration Hamiltonian H^{u_0} and a local perturbation due to the flipped link variable u^z_0:

$$\mathcal{H}^{0,z} = \mathcal{H}^{u_0} - 2iK c^A_0 c^B_0. \tag{10}$$

The Hamiltonian with a single flipped link $\mathcal{H}^{0,z}$ can be written in terms of the excitations of the trivial link configuration:

$$\mathcal{H}^{0,z} = \mathcal{H}^{u_0} + 2|K| U^{u_0}_{0,k} V^{u_0}_{0,k'} \left(\eta^{u_0}_k + \eta^{u_0\dagger}_k\right)\left(\eta^{u_0\dagger}_{k'} - \eta^{u_0}_{k'}\right), \tag{11}$$

where a sum over indices k and k' is understood. Written in this form the Hamiltonian is independent of the sign of the Kitaev coupling. This means that the ground state $|0^{0,z}\rangle$ will have the same form for both signs of the Kitaev interaction, when expressed in terms of the creation and annihilation operators η^{u_0},$\eta^{u_0\dagger}$ and the ground state of the trivial flux configuration $|0^{u_0}\rangle$ [see Eq. (13) below]. It is important to emphaszse that the ground state wave function is not the same for both signs of the Kitaev interaction, as the dependence on the sign of K has been included in the definition of η^{u_0}. The difference between eigenstates for different signs of the Kitaev interaction becomes important when non-Kitaev interactions are included in the Hamiltonian.

Using the singular value decomposition of M^u in Eq. (5), the Majorana operators $C^{u,A}$ and $C^{u,B}$ on the A and B sublattices, which diagonalize each Hamiltonian, may be related by real orthogonal transformations:

$$C^{(0,z),A} = UC^{u_0,A}, \quad C^{(0,z),B} = VC^{u_0,B},$$

where $U = U^{(0,z),T} U^{u_0}$ and $V = V^{(0,z),T} V^{u_0}$. The relation between the complex fermions $\eta^{(0,z)}$ and η^{u_0}, defined in Eq. (7), is given by a real transformation:

$$\begin{pmatrix} \eta^{(0,z)} \\ \eta^{(0,z)\dagger} \end{pmatrix} = \begin{pmatrix} X & Y \\ Y & X \end{pmatrix} \begin{pmatrix} \eta^{u_0} \\ \eta^{u_0\dagger} \end{pmatrix}, \tag{12}$$

where $X = (U+V)/2$ and $Y = (U-V)/2$. The corresponding matter sector ground states are related by [23]

$$|0^{0,z}\rangle = \langle 0^{u_0}|0^{0,z}\rangle \exp\left(-\frac{1}{2}\sum_{k,k'} \eta^{u_0\dagger}_k Z_{k,k'} \eta^{u_0\dagger}_{k'}\right) |0^{u_0}\rangle, \tag{13}$$

where $Z = X^{-1}Y$ is a real antisymmetric matrix. As Z is real antisymmetric it may be decomposed by a real orthogonal

matrix Q into the form

$$Z = Q \begin{pmatrix} & -t_1 & & & \\ t_1 & & & & \\ & & & -t_2 & \\ & & t_2 & & \\ & & & & \ddots \end{pmatrix} Q^T, \tag{14}$$

where the nonzero elements $t_j = \tan(\theta_j/2)$ are real numbers, and $|\tan(\theta_j/2)|$ correspond to the singular values of Z. The orthogonal matrix Q can be used to define a canonical transformation to a new set of creation operators $\bar{\eta}_j^\dagger = Q_{jk}^T \eta_k^\dagger$. The transformed creation operators corresponding to nonzero $\tan(\theta_j/2)$ are paired, with the two operators in the pair labeled $\bar{\eta}_{j,a}^{u_0\dagger}, \bar{\eta}_{j,b}^{u_0\dagger}$. They are not unique, as the following transformation leaves the relation between ground states unchanged:

$$\begin{pmatrix} \bar{\eta}_a^\dagger \\ \bar{\eta}_b^\dagger \end{pmatrix} \to \exp(i\phi\sigma^y) \begin{pmatrix} \bar{\eta}_a^\dagger \\ \bar{\eta}_b^\dagger \end{pmatrix}, \quad \phi \in \mathbb{R}. \tag{15}$$

The operator relating ground states may then be written in terms of the transformed operators as

$$\exp\left(-\frac{1}{2}\sum_{k,k'} \eta_k^{u_0\dagger} Z_{k,k'} \eta_{k'}^{u_0\dagger}\right) = \exp\left(\sum_j t_j \bar{\eta}_{j,a}^{u_0\dagger} \bar{\eta}_{j,b}^{u_0\dagger}\right) = \prod_j \left[1 + \tan(\theta_j/2) \bar{\eta}_{j,a}^{u_0\dagger} \bar{\eta}_{j,b}^{u_0\dagger}\right]. \tag{16}$$

Here, sums and products are over the pairs of nonzero singular values of Z.

A single flipped bond variable is a local perturbation of the flux-free Hamiltonian $\mathcal{H}^{u_0}$ and the change to the ground state as described by Z is localized around the vison pair [16]. This means that there are very few nonzero values of $\tan(\theta_j/2)$, with the corresponding fermion operators localized around the vison pair. The change to the ground state may be approximated as being due solely to the largest term such that the operator relating the ground states of the two sectors is

$$|0^{0,z}\rangle = \langle 0^{u_0}|0^{0,z}\rangle \exp\left(-\frac{1}{2}\sum_{k,k'} \eta_k^{u_0\dagger} Z_{k,k'} \eta_{k'}^{u_0\dagger}\right)|0^{u_0}\rangle \approx \left[\cos(\theta/2) + \sin(\theta/2)\bar{\eta}_a^{u_0\dagger}\bar{\eta}_b^{u_0\dagger}\right]|0^{u_0}\rangle. \tag{17}$$

The matrix Z may be determined exactly numerically for finite-size systems using exact diagonalization of the matter sector Hamiltonians for the two different flux configurations, as has been carried out in previous works on vison dynamics in perturbed Kitaev models [16–19]. However, by approximating Z by only its largest singular values, the relation between ground states is simple enough to find an approximate explicit expression. This allows calculations on much larger lattices than can be directly studied using exact diagonalization, and is a simple starting point for further study of vison pair excitations in perturbed Kitaev models. The approximation in Eq. (17) will be the ansatz for a variational calculation of the matter fermion ground state in the presence of a neighboring pair of visons.

Variational approximation of the vison pair state

The ansatz for the ground state of the matter sector Hamiltonian for a single flipped bond is

$$|\bar{0}^{0,z}\rangle = (\cos(\theta/2) + \sin(\theta/2)\bar{\eta}_a^\dagger \bar{\eta}_b^\dagger)|0^{u_0}\rangle. \tag{18}$$

The operator $\bar{\eta}_a^\dagger$ can be written in the basis of the eigenstate operators of $\mathcal{H}^{u_0}$:

$$\bar{\eta}_a^\dagger = \sum_{\boldsymbol{k}\in \mathrm{BZ}/2} \left(a_{\boldsymbol{k},+}\eta_{\boldsymbol{k},+}^{u_0,\dagger} + a_{\boldsymbol{k},-}\eta_{\boldsymbol{k},-}^{u_0,\dagger}\right) = \sum_{\boldsymbol{k}\in \mathrm{BZ}} a_{\boldsymbol{k}}\eta_{\boldsymbol{k}}^{u_0,\dagger},$$
$$\bar{\eta}_b^\dagger = \sum_{\boldsymbol{k}\in \mathrm{BZ}/2} \left(b_{\boldsymbol{k},+}\eta_{\boldsymbol{k},+}^{u_0,\dagger} + b_{\boldsymbol{k},-}\eta_{\boldsymbol{k},-}^{u_0,\dagger}\right) = \sum_{\boldsymbol{k}\in \mathrm{BZ}} b_{\boldsymbol{k}}\eta_{\boldsymbol{k}}^{u_0,\dagger},$$

where $a_{\boldsymbol{k},+}, a_{\boldsymbol{k},-}$ are real and $a_{\boldsymbol{k}} = (a_{\boldsymbol{k}+} + i a_{\boldsymbol{k},-})/\sqrt{2}$ are complex and satisfy $a_{-\boldsymbol{k}} = a_{\boldsymbol{k}}^*$. The expansion coefficients $b_{\boldsymbol{k}}$ satisfy analogous conditions. The eigenstate operators $\eta_{\boldsymbol{k}}^{u_0}$ from Eq. (8) and complex parameters $a_{\boldsymbol{k}}, b_{\boldsymbol{k}}$ are used in order to make the following calculation more compact. The parameters $a_{\boldsymbol{k}}$, $b_{\boldsymbol{k}}$, and θ are to be determined by minimization of the ground state energy expectation value. Note that the parameters $a_{\boldsymbol{k}}, b_{\boldsymbol{k}}$ are constrained by their normalization $\sum_{\boldsymbol{k}} |a_{\boldsymbol{k}}|^2 = \sum_{\boldsymbol{k}} |b_{\boldsymbol{k}}|^2 = 1$ and orthogonality $\sum_{\boldsymbol{k}} a_{\boldsymbol{k}} b_{\boldsymbol{k}}^* = 0$, with the constraints enforced by Lagrange multipliers Λ_a, Λ_b, and Λ_{ab}, respectively.

We performed the minimization of the expectation value for the ground state energy $\bar{E}^{0,z} = \langle \bar{0}^{0,z}| \mathcal{H}^{0,z} |\bar{0}^{0,z}\rangle$ with respect to each of the variational parameters and solved the resulting equations in a case where $\Lambda_{ab} = 0$. This is always possible for a suitable value of ϕ in Eq. (15), and this is a convenient choice as the resulting equations for $a_{\boldsymbol{k}}$ and $b_{\boldsymbol{k}}$ are decoupled. The details of the solution are given in Appendix A. For the most general case of a vison pair at site $\boldsymbol{r}$ with orientation α the optimized parameters are

$$a_{\boldsymbol{k}}^{(\boldsymbol{r},\alpha)} = \frac{A_a}{\sqrt{N}} \frac{1 + e^{i\varphi_{\boldsymbol{k}} + i\boldsymbol{k}\cdot(\boldsymbol{r}_\alpha - \boldsymbol{r}_z)}}{\Lambda_a + |\Delta_{\boldsymbol{k}}|} e^{i\boldsymbol{k}\cdot\boldsymbol{r}}, \tag{19}$$

$$b_{\boldsymbol{k}}^{(\boldsymbol{r},\alpha)} = \frac{A_b}{\sqrt{N}} \frac{e^{i\varphi_{\boldsymbol{k}} + i\boldsymbol{k}\cdot(\boldsymbol{r}_\alpha - \boldsymbol{r}_z)} - 1}{\Lambda_b + |\Delta_{\boldsymbol{k}}|} e^{i\boldsymbol{k}\cdot\boldsymbol{r}} \tag{20}$$

with

$$\Lambda_a = 1.5384,$$
$$\Lambda_b = 0.2995,$$
$$\theta = 0.9565.$$

The energy of the vison pair above the ground state in this approximation is given by $\bar{\Delta} = \bar{E}^{0,z} - \langle 0^{u_0}| \mathcal{H}^{u_0} |0^{u_0}\rangle \approx 0.272|K|$, which is within 3% of the exact result calculated analytically, $\Delta = 0.263|K|$ [24].

IV. COMPARISON TO EXACT RESULTS

We evaluate the accuracy of the optimized approximate ground state by calculating physical quantities and comparing them to the results of exact diagonalization performed on finite lattices [16,17]. While the ground state is calculated for a particular link configuration, and is therefore not gauge invariant, it can still be used to calculate physical quantities by acting on it with the projection operator in Eq. (2). Depending on the boundary conditions [25], the projection operator will

annihilate states with either even or odd fermion parity. In cases in which a lone vison pair would be annihilated, the projector may be modified to simulate a matter fermion at a large distance from the vison pair, which reverses the overall fermion parity of the state so that the state is no longer annihilated [16].

A. Link energy around vison pairs

We start by calculating the change in link energy, defined as $\varepsilon_{\boldsymbol{r}}^{\alpha} = K\langle\sigma_{\boldsymbol{r}}^{\alpha}\sigma_{\boldsymbol{r}+\boldsymbol{r}_\alpha}^{\alpha}\rangle = K\langle\hat{u}_{\boldsymbol{r}}^{\alpha} ic_{\boldsymbol{r}}c_{\boldsymbol{r}+\boldsymbol{r}_\alpha}\rangle$, between the ground states with and without the vison pair. This quantity provides a direct test for the performance of our optimized approximation. Figure 2(a) shows the change in link energy calculated using the optimized approximation. The majority of the change in link energy is localized on the x and y links neighboring the visons, and on the flipped z link itself. The difference between the link energy calculated using exact diagonalization for a finite lattice of 58×58 unit cells and the optimized approximation is shown in Fig. 2(b). Note the difference in scale between Figs. 2(a) and 2(b). The largest differences are on the z bonds neighboring the plaquette. In the central region where the majority of the energy is localized, the relative error is approximately 5%. This allows us to conclude that the approximation is robust and we expect it to be able to produce reliable results. Furthermore, it can be consistently improved by including further terms coming from the second, third, etc., largest singular values of Z in the variational Ansatz (18).

B. Hopping of vison pairs

Zhang *et al.* [16] showed that the hopping parameters for vison pairs can be related to matrix elements of matter sector ground states for fixed link configurations. The hopping parameter of vison pairs in the presence of a perturbing Heisenberg interaction $\mathcal{H}^J = J\sum_{\boldsymbol{r},\alpha}\sigma_{\boldsymbol{r}}\cdot\sigma_{\boldsymbol{r}+\boldsymbol{r}_\alpha}$ is [16]

$$\begin{aligned}\mathcal{T}^J &= \langle \boldsymbol{r}+\mathbf{a}_1, z|\,\mathcal{H}^J\,|\boldsymbol{r}, z\rangle \\ &= J\big(\langle 0^{\mathbf{a}_1,z}|0^{0,z}\rangle + \langle 0^{\mathbf{a}_1,z}|\,ic_{\mathbf{a}_1}^{A}c_0^{B}\,|0^{0,z}\rangle\big). \end{aligned} \tag{21}$$

This was calculated using exact diagonalization on finite-size lattices and extrapolating to the limit of infinite-size lattices [16]. The dependence on the sign of the Kitaev coupling of the second term is clear once matrix elements are expressed in terms of creation and annihilation operators of matter fermion excitations for a given link configuration:

$$\begin{aligned}&\langle 0^{\mathbf{a}_1,z}|\,ic_{\mathbf{a}_1}^{A}c_0^{B}\,|0^{0,z}\rangle \\ &\quad= \frac{K}{|K|}U_{\mathbf{a}_1,k}^{u_0}V_{0,k'}^{u_0}\,\langle 0^{\mathbf{a}_1,z}|\left(\eta_k^{u_0}+\eta_k^{u_0\dagger}\right)\left(\eta_{k'}^{u_0}-\eta_{k'}^{u_0\dagger}\right)|0^{0,z}\rangle\,.\end{aligned}$$

Once the matrix elements are expressed using matter fermion excitation operators they are independent of the sign of K, so the second term in Eq. (21) differs in sign between antiferromagnetic (AFM) and ferromagnetic (FM) Kitaev models, as concluded in [16]. These matrix elements may also be calculated using the approximate ground states with the optimized parameters. The details of the calculation are given in Appendix B. For AFM Kitaev coupling our approximation gives $\mathcal{T}^J = 1.496$, compared to $\mathcal{T}^J \to 1.470J$ from exact diagonalization [16]. For ferromagnetic coupling, as noted in [16], there is destructive interference between the two terms. Our approximation gives $\mathcal{T}^J = 0.0991J$ whereas the extrapolation of exact diagonalization results gives $\mathcal{T}^J \to 0.0938J$. The relative error is approximately 6%, which denotes a good performance of the approximate method, particularly as this quantity is sensitive to small changes in the ground state due to the destructive interference between the two terms.

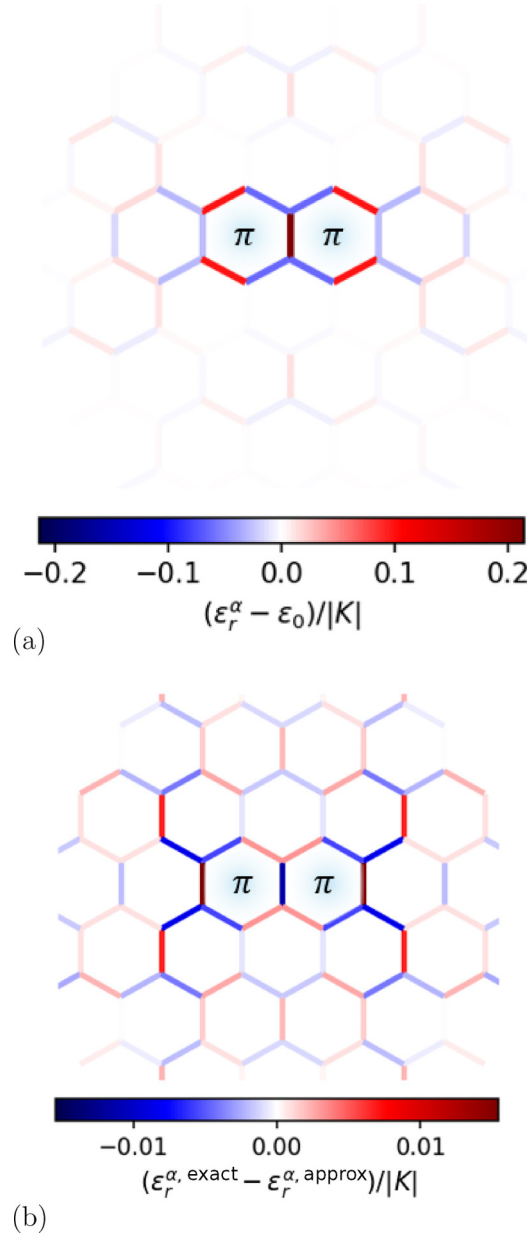


FIG. 2. Panel (a): The change in link energy around the vison pair calculated using the variational Ansatz in Eq. (18). Panel (b): The difference between the link energies calculated using the variational Ansatz (18) and exact diagonalization on a 58×58 lattice with periodic boundaries [26]. Note the change in scale compared to Panel (a) by about one order of magnitude. In both panels, visons are located on the shaded plaquettes marked with "π".

In Appendix B we have also calculated hopping due to the off-diagonal symmetric exchange $\mathcal{H}^\Gamma = \Gamma\sum_{\boldsymbol{r}}\sum_{\alpha\neq\beta\neq\gamma}\sigma_{\boldsymbol{r}}^{\beta}\sigma_{\boldsymbol{r}+\boldsymbol{r}_\alpha}^{\gamma}$, and the Zeeman coupling

$\mathcal{H}^h = h\sum_{\boldsymbol{r},\alpha}\sigma^\alpha_{\boldsymbol{r}}$. Our results, compared to those extrapolated from exact diagonalization of finite lattices [16,17], are reported in Table I in units of the respective coupling constants.

V. DISCUSSION

In this work we have shown that the change to the matter fermion ground state due to the presence of a vison pair in a generalized Kitaev model may be approximated by a simple expression. Using the variational method we developed here, we obtained an analytical expression for the vison pair state in terms of the eigenstates of the vison-free Hamiltonian.

The approximate state was used to calculate the link energy and vison hopping amplitudes that we then compared to the results of exact diagonalization. We have shown that the approximate state is successful in capturing the main effect of the vison pair–spinon interaction to within ≈6%. A more precise determination of the matrix elements requires including more variational parameters in the ansatz corresponding to the smaller singular values, or resorting to exact diagonalization.

The power of the method we have developed hinges on the possibility to explicitly construct a simple expression for the vison pair state, Eq. (18). This is achieved by retaining only the contribution of the largest pair of singular values of Z to Eq. (16). More precise results may be obtained by including further terms coming from the second, third, etc., largest pairs of singular values of Z in the variational ansatz. However, this complicates the minimization and it is beyond the scope of the present work.

The variational method we have developed could be used to go beyond numerical calculations in studies of, e.g., magnon-like bound states formed between vison pairs and spinons or to describe the ground state of the extended Kitaev model [1]. The latter includes time-reversal symmetry breaking three-spin interactions that emerge in weak magnetic fields. It can also in principle be extended to ground states of more complicated vison configurations. For example to "open pairs," in which visons are separated by longer chains of flipped link variables. The study of these more complicated cases is, however, beyond the scope of the present work.

If Z presents too many singular values that need to be retained, a direct application of the method could become impractical due to the number of variational parameters needed to accurately describe the state. In these cases, a possible solution could be breaking too long chains into shorter ones, i.e., by considering changes to the ground state induced by flipping a smaller number of links. These could likely be written in terms of a few variational parameters onto which minimization can be performed. Repeating the process, it could then be possible to build up and approximate the ground state of longer chains of flipped bonds. Further work, beyond the scope of the present paper, is needed to generalize our method to these cases.

ACKNOWLEDGMENTS

We acknowledge support from the European Commission under the EU Horizon 2020 MSCA-RISE-2019 program (Project 873028 HYDROTRONICS), from the Leverhulme Trust under the Grant Agreement No. RPG-2023-253 and from the Engineering and Physical Sciences Research Council Grant No. EP/W524347/1 (Project 2856485).

DATA AVAILABILITY

The data that support the findings of this article are openly available [26].

APPENDIX A: MINIMIZATION OF THE GROUND STATE ENERGY

The optimized parameters for the variational ansatz given in Eq. (18) are found using the standard variational method, i.e., by writing down the ground state energy expectation in terms of the variational parameters and minimizing with respect to them. The expectation value for the ground state energy $\bar{E}^{0,z} = \langle\bar{0}^{0,z}|\,\mathcal{H}^{0,z}\,|\bar{0}^{0,z}\rangle$ in terms of the variational parameters is given by Eq. (A1):

$$\begin{aligned}\bar{E}^{0,z} = {}& \langle 0^{u_0}|\,H^{0z}\,|0^{u_0}\rangle \\ & + 2\sin^2(\theta/2)\sum_{\boldsymbol{k}}|\Delta_{\boldsymbol{k}}|(|b_{\boldsymbol{k}}|^2+|a_{\boldsymbol{k}}|^2) \\ & + 2\sin(\theta)[(Ub)_0(Va)_0-(Ua)_0(Vb)_0] \\ & - 4\sin^2(\theta/2)[(Ua)_0(Va)_0+(Ub)_0(Vb)_0] \\ & + 2\sin^2(\theta/2)\Lambda_a\left(\sum_{\boldsymbol{k}}|a_{\boldsymbol{k}}|^2-1\right) \\ & + 2\sin^2(\theta/2)\Lambda_b\left(\sum_{\boldsymbol{k}}|b_{\boldsymbol{k}}|^2-1\right) \\ & + \Lambda_{ab}\left(\sum_{\boldsymbol{k}}a_{\boldsymbol{k}}b^*_{\boldsymbol{k}}\right),\end{aligned} \tag{A1}$$

where

$$\begin{aligned}(Ua)_0 &= \frac{1}{\sqrt{N}}\sum_{\boldsymbol{k}\in\mathrm{BZ}}a_{\boldsymbol{k}}, \\ (Va)_0 &= \frac{1}{\sqrt{N}}\sum_{\boldsymbol{k}\in\mathrm{BZ}}a_{\boldsymbol{k}}e^{-i\varphi_{\boldsymbol{k}}}.\end{aligned}$$

There are analogous expressions for $(Ub)_0$ and $(Vb)_0$. Differentiating $\bar{E}^{0,z}$ with respect to $a_{\boldsymbol{k}}$ and $b_{\boldsymbol{k}}$ gives

$$\begin{aligned}& 4\sin^2(\theta/2)(|\Delta_{\boldsymbol{k}}|+\Lambda_a)a^*_{\boldsymbol{k}}+\Lambda_{ab}b^*_{\boldsymbol{k}} \\ & = \frac{4}{\sqrt{N}}\sin^2(\theta/2)[(Ua)_0e^{-i\varphi_{\boldsymbol{k}}}+(Va)_0] \\ & \quad - \frac{2}{\sqrt{N}}\sin(\theta)[(Ub)_0e^{-i\varphi_{\boldsymbol{k}}}-(Vb)_0],\end{aligned} \tag{A2}$$

and

$$\begin{aligned}& 4\sin^2(\theta/2)(|\Delta_{\boldsymbol{k}}|+\Lambda_b)b^*_{\boldsymbol{k}}+\Lambda_{ab}a^*_{\boldsymbol{k}} \\ & = \frac{4}{\sqrt{N}}\sin^2(\theta/2)[(Ub)_0e^{-i\varphi_{\boldsymbol{k}}}+(Vb)_0] \\ & \quad + \frac{2}{\sqrt{N}}\sin(\theta)[(Ua)_0e^{-i\varphi_{\boldsymbol{k}}}-(Va)_0].\end{aligned} \tag{A3}$$

Multiplying Eq. (A2) by $b_{\boldsymbol{k}}$ and summing over the Brillouin zone gives an equation for the Lagrange multiplier Λ_{ab}:

$$4\sin^2(\theta/2)\sum_{\boldsymbol{k}} b_{\boldsymbol{k}}|\Delta_{\boldsymbol{k}}|a^*_{\boldsymbol{k}} + \Lambda_{ab} = 4\sin^2(\theta/2)[(Ua)_0(Vb)_0 + (Va)_0(Ub)_0]. \tag{A4}$$

We will seek a solution to the equations with $\Lambda_{ab} = 0$. This is possible by exploiting the $U(1)$ redundancy of Eq. (15) to require that $(Ua)_0 = (Va)_0$ and $(Ub)_0 = -(Vb)_0$. Enforcing this ensures $\sum_{\boldsymbol{k}} |\Delta_{\boldsymbol{k}}| b^*_{\boldsymbol{k}} a_{\boldsymbol{k}} = 0$ is also satisfied. A solution of this form has

$$a_{\boldsymbol{k}} = \frac{A_a}{\sqrt{N}} \frac{1 + e^{i\varphi_{\boldsymbol{k}}}}{\Lambda_a + |\Delta_{\boldsymbol{k}}|} \tag{A5}$$

and

$$b_{\boldsymbol{k}} = \frac{A_b}{\sqrt{N}} \frac{e^{i\varphi_{\boldsymbol{k}}} - 1}{\Lambda_b + |\Delta_{\boldsymbol{k}}|}, \tag{A6}$$

with

$$A_a = (Ua)_0 - (Ub)_0\cot(\theta/2), \tag{A7}$$

$$A_b = (Ub)_0 + (Ua)_0\cot(\theta/2). \tag{A8}$$

The quantities A_a and A_b may be related to Λ_a and Λ_b by using the normalization constraints. Furthermore, Eqs. (A7) and (A8) allow Λ_b and θ to be determined from Λ_a. Minimizing $\bar{E}^{0,z}$ with respect to θ gives

$$\sin(\theta)\sum_{\boldsymbol{k}} |\Delta_{\boldsymbol{k}}|(|b_{\boldsymbol{k}}|^2 + |a_{\boldsymbol{k}}|^2) + 4\cos(\theta)(Ua)_0(Ub)_0 = 2\sin(\theta)\left[(Ua)_0^2 - (Ub)_0^2\right]. \tag{A9}$$

Using Eqs. (A5) and (A6),

$$\sum_{\boldsymbol{k}} |\Delta_{\boldsymbol{k}}||a_{\boldsymbol{k}}|^2 = 2A_a(Ua)_0 - \Lambda_a = 2(Ua)_0^2 - 2(Ua)_0(Ub)_0\cot(\theta/2) - \Lambda_a,$$

$$\sum_{\boldsymbol{k}} |\Delta_{\boldsymbol{k}}||b_{\boldsymbol{k}}|^2 = -2A_b(Ub)_0 - \Lambda_b = -2(Ub)_0^2 - 2(Ua)_0(Ub)_0\cot(\theta/2) - \Lambda_b.$$

Substituting these into Eq. (A9) and simplifying gives

$$\Lambda_a + \Lambda_b = -4(Ua)_0(Ub)_0\csc(\theta). \tag{A10}$$

Both sides of the equation may be regarded as functions of Λ_a. Solving numerically for Λ_a, and using Eqs. (A7) and (A8) to determine Λ_b and θ gives

$$\Lambda_a = 1.5396,$$
$$\Lambda_b = 0.2995,$$
$$\theta = 0.9561.$$

This may be generalized to an arbitrary vison pair site $\boldsymbol{r}$ and orientation α to give the result stated in Eqs. (19) and (20) in the main text.

APPENDIX B: CALCULATION OF HOPPING PARAMETERS

The matrix elements that must be calculated to calculate the hopping parameters of vison pairs have the general form

$$\langle 0^{\boldsymbol{R},\alpha}|0^{\boldsymbol{R}',\beta}\rangle = \cos^2(\theta/2) + \sin^2(\theta/2)[(a^{\boldsymbol{R},\alpha}\cdot a^{\boldsymbol{R}',\beta})(b^{\boldsymbol{R},\alpha}\cdot b^{\boldsymbol{R}',\beta}) - (a^{\boldsymbol{R},\alpha}\cdot b^{\boldsymbol{R}',\beta})(b^{\boldsymbol{R},\alpha}\cdot a^{\boldsymbol{R}',\beta})], \tag{B1}$$

$$\begin{aligned}\frac{K}{|K|}\langle 0^{\boldsymbol{R},\alpha}|\, ic^A_{\boldsymbol{r}}c^B_{\boldsymbol{r}'}\,|0^{\boldsymbol{R}',\beta}\rangle = &-(U^{u_0}V^{u_0T})_{\boldsymbol{r},\boldsymbol{r}'}\langle 0^{\boldsymbol{R},\alpha}|0^{\boldsymbol{R}',\beta}\rangle \\ &+\frac{1}{2}\sin(\theta)((Ub^{\boldsymbol{R},\alpha})_{\boldsymbol{r}}(Va^{\boldsymbol{R},\alpha})_{\boldsymbol{r}'} - (Vb^{\boldsymbol{R},\alpha})_{\boldsymbol{r}'}(Ua^{\boldsymbol{R},\alpha})_{\boldsymbol{r}}) \\ &+\frac{1}{2}\sin(\theta)(Ub^{\boldsymbol{R}',\beta})_{\boldsymbol{r}}(Va^{\boldsymbol{R}',\beta})_{\boldsymbol{r}'} - (Vb^{\boldsymbol{R}',\beta})_{\boldsymbol{r}'}(Ua^{\boldsymbol{R}',\beta})_{\boldsymbol{r}}) \\ &+\sin^2(\theta/2)((b^{\boldsymbol{R},\alpha}\cdot b^{\boldsymbol{R}',\beta})[(Ua^{\boldsymbol{R},\alpha})_{\boldsymbol{r}}(Va^{\boldsymbol{R}',\beta})_{\boldsymbol{r}'} + (Va^{\boldsymbol{R},\alpha})_{\boldsymbol{r}'}(Ua^{\boldsymbol{R}',\beta})_{\boldsymbol{r}}] \\ &+(a^{\boldsymbol{R},\alpha}\cdot a^{\boldsymbol{R}',\beta})[(Ub^{\boldsymbol{R},\alpha})_{\boldsymbol{r}}(Vb^{\boldsymbol{R}',\beta})_{\boldsymbol{r}'} + (Vb^{\boldsymbol{R},\alpha})_{\boldsymbol{r}'}(Ub^{\boldsymbol{R}',\beta})_{\boldsymbol{r}}] \\ &-(a^{\boldsymbol{R},\alpha}\cdot b^{\boldsymbol{R}',\beta})[(Ub^{\boldsymbol{R},\alpha})_{\boldsymbol{r}}(Va^{\boldsymbol{R}',\beta})_{\boldsymbol{r}'} + (Vb^{\boldsymbol{R},\alpha})_{\boldsymbol{r}'}(Ua^{\boldsymbol{R}',\beta})_{\boldsymbol{r}}] \\ &-(b^{\boldsymbol{R},\alpha}\cdot a^{\boldsymbol{R}',\beta})[(Ua^{\boldsymbol{R},\alpha})_{\boldsymbol{r}}(Vb^{\boldsymbol{R}',\beta})_{\boldsymbol{r}'} + (Va^{\boldsymbol{R},\alpha})_{\boldsymbol{r}'}(Ub^{\boldsymbol{R}',\beta})_{\boldsymbol{r}}]),\end{aligned} \tag{B2}$$

where

$$(Ua^{(\boldsymbol{R},\alpha)})_{\boldsymbol{r}} = \frac{A_a}{N}\sum_{\boldsymbol{k}\in\mathrm{BZ}} e^{i\boldsymbol{k}\cdot(\boldsymbol{r}-\boldsymbol{R})}\frac{1 + e^{i[\boldsymbol{k}\cdot(\boldsymbol{r}_z-\boldsymbol{r}_\alpha)-\varphi_{\boldsymbol{k}}]}}{\Lambda_a + |\Delta_{\boldsymbol{k}}|}, \tag{B3}$$

$$(Va^{(\boldsymbol{R},\alpha)})_{\boldsymbol{r}} = (Ua^{(\boldsymbol{R},\alpha)})_{2\boldsymbol{R}-\boldsymbol{r}+\boldsymbol{r}_\alpha-\boldsymbol{r}_z}, \tag{B4}$$

$$(Ub^{(\boldsymbol{R},\alpha)})_{\boldsymbol{r}} = \frac{A_b}{N}\sum_{\boldsymbol{k}\in\mathrm{BZ}} e^{i\boldsymbol{k}\cdot(\boldsymbol{r}-\boldsymbol{R})}\frac{1 - e^{i[\boldsymbol{k}\cdot(\boldsymbol{r}_z-\boldsymbol{r}_\alpha)-\varphi_{\boldsymbol{k}}]}}{\Lambda_b + |\Delta_{\boldsymbol{k}}|}, \tag{B5}$$

$$(Vb^{(\boldsymbol{R},\alpha)})_{\boldsymbol{r}} = -(Ub^{(\boldsymbol{R},\alpha)})_{2\boldsymbol{R}-\boldsymbol{r}+\boldsymbol{r}_\alpha-\boldsymbol{r}_z}, \tag{B6}$$

$$(a^{(\boldsymbol{R},\alpha)}\cdot a^{(\boldsymbol{R}',\beta)}) = \frac{A_a^2}{N}\sum_{\boldsymbol{k}\in \mathrm{BZ}} e^{i\boldsymbol{k}\cdot(\boldsymbol{R}-\boldsymbol{R}')}\frac{1+e^{i\boldsymbol{k}\cdot(\boldsymbol{r}_\alpha-\boldsymbol{r}_z)+\varphi_{\boldsymbol{k}}}+e^{-i\boldsymbol{k}\cdot(\boldsymbol{r}_\beta-\boldsymbol{r}_z)-\varphi_{\boldsymbol{k}}}+e^{i\boldsymbol{k}\cdot(\boldsymbol{r}_\alpha-\boldsymbol{r}_\beta)}}{(\Lambda_a+|\Delta_{\boldsymbol{k}}|)^2}, \tag{B7}$$

$$(b^{(\boldsymbol{R},\alpha)}\cdot b^{(\boldsymbol{R}',\beta)}) = \frac{A_b^2}{N}\sum_{\boldsymbol{k}\in \mathrm{BZ}} e^{i\boldsymbol{k}\cdot(\boldsymbol{R}-\boldsymbol{R}')}\frac{1-e^{i\boldsymbol{k}\cdot(\boldsymbol{r}_\alpha-\boldsymbol{r}_z)+\varphi_{\boldsymbol{k}}}-e^{-i\boldsymbol{k}\cdot(\boldsymbol{r}_\beta-\boldsymbol{r}_z)-\varphi_{\boldsymbol{k}}}+e^{i\boldsymbol{k}\cdot(\boldsymbol{r}_\alpha-\boldsymbol{r}_\beta)}}{(\Lambda_b+E_{\boldsymbol{k}})^2}, \tag{B8}$$

$$(a^{(\boldsymbol{R},\alpha)}\cdot b^{(\boldsymbol{R}',\beta)}) = \frac{A_bA_a}{N}\sum_{\boldsymbol{k}\in \mathrm{BZ}} e^{i\boldsymbol{k}\cdot(\boldsymbol{R}-\boldsymbol{R}')}\frac{1+e^{i\boldsymbol{k}\cdot(\boldsymbol{r}_\alpha-\boldsymbol{r}_z)+\varphi_{\boldsymbol{k}}}-e^{-i\boldsymbol{k}\cdot(\boldsymbol{r}_\beta-\boldsymbol{r}_z)-\varphi_{\boldsymbol{k}}}-e^{i\boldsymbol{k}\cdot(\boldsymbol{r}_\alpha-\boldsymbol{r}_\beta)}}{(\Lambda_a+|\Delta_{\boldsymbol{k}}|)(\Lambda_b+|\Delta_{\boldsymbol{k}}|)}. \tag{B9}$$

1. Heisenberg interaction

The Heisenberg interaction Hamiltonian is given by

$$\mathcal{H}^J = J\sum_{\substack{\boldsymbol{r}\in A\\ \alpha=z,y,z}} \sigma_{\boldsymbol{r}}\cdot\sigma_{\boldsymbol{r}+\boldsymbol{r}_\alpha}.$$

Using the expression from Ref. [16], the hopping parameter for vison pairs in the presence of Heisenberg interactions is as follows:

$$\begin{aligned}\mathcal{T}^J &= \langle \boldsymbol{R}+\mathbf{a}_1,z|\,\mathcal{H}^J\,|\boldsymbol{R},z\rangle\\ &= J\big(\langle 0^{\boldsymbol{R}+\mathbf{a}_1,z}|0^{\boldsymbol{R},z}\rangle + \langle 0^{\boldsymbol{R}+\mathbf{a}_1,z}|\,ic^A_{\boldsymbol{R}+\mathbf{a}_1}c^B_{\boldsymbol{R}}\,|0^{\boldsymbol{R},z}\rangle\big).\end{aligned}$$

Using the general formulas, Eqs. (B1) and (B2),

$$\langle 0^{\boldsymbol{R}+\mathbf{a}_1,z}|0^{\boldsymbol{R},z}\rangle = 0.7977,$$
$$\langle 0^{\boldsymbol{R}+\mathbf{a}_1,z}|\,ic^A_{\boldsymbol{R}+\mathbf{a}_1}c^B_{\boldsymbol{R}}\,|0^{\boldsymbol{R},z}\rangle = -0.6986\,\mathrm{sgn}(K).$$

2. Gamma interactions

The Gamma interaction Hamiltonian is given by

$$\mathcal{H}^\Gamma = \Gamma\sum_{\substack{\boldsymbol{r}\in A\\ \alpha\neq\beta\neq\gamma}} \sigma^\beta_{\boldsymbol{r}}\sigma^\gamma_{\boldsymbol{r}+\boldsymbol{r}_\alpha}. \tag{B10}$$

The hopping parameter for vison pairs due to Gamma interactions [16] is

$$\mathcal{T}^\Gamma = \Gamma\big(\langle 0^{\boldsymbol{R}+\mathbf{a}_1,y}|\,ic^A_{\boldsymbol{R}+\mathbf{a}_1}c^B_{\boldsymbol{R}}\,|0^{\boldsymbol{R},z}\rangle - \langle 0^{\boldsymbol{R}+\mathbf{a}_1,y}|0^{\boldsymbol{R},z}\rangle\big). \tag{B11}$$

Using the general formulas, Eqs. (B1) and (B2),

$$\langle 0^{\boldsymbol{R}+\mathbf{a}_1,y}|0^{\boldsymbol{R},z}\rangle = 0.8220,$$
$$\langle 0^{\boldsymbol{R}+\mathbf{a}_1,y}|\,ic^A_{\boldsymbol{R}+\mathbf{a}_1}c^B_{\boldsymbol{R}}\,|0^{\boldsymbol{R},z}\rangle = -0.6411\,\mathrm{sgn}(K).$$

3. Zeeman interactions

The Zeeman interaction for a uniform magnetic field h in the [1,1,1] direction is given by

$$\mathcal{H}^h = h\sum_{\substack{\boldsymbol{r}\in A,B\\ \alpha=x,y,z}} \sigma^\alpha_{\boldsymbol{r}}. \tag{B12}$$

The hopping parameter for vison pairs due to the Zeeman interaction at first order is given by

$$\mathcal{T}^h = ih\big(\langle 0^{\boldsymbol{R},\beta}|0^{\boldsymbol{R},\alpha}\rangle - \langle 0^{\boldsymbol{R},\beta}|\,ic^A_{\boldsymbol{R}}c^B_{\boldsymbol{R}+\boldsymbol{r}_\gamma-\boldsymbol{r}_z}\,|0^{\boldsymbol{R},\alpha}\rangle\big). \tag{B13}$$

Note that in this calculation we have neglected the change to the matter sector Hamiltonian due to the Haldane mass term that is induced at third order in the magnetic field strength [1]. Inclusion of these effects is open for further work. Using the general formulas, Eqs. (B1) and (B2),

$$\langle 0^{\boldsymbol{R},\beta}|0^{\boldsymbol{R},\alpha}\rangle = 0.7184,$$
$$\langle 0^{\boldsymbol{R},\beta}|\,ic^A_{\boldsymbol{R}}c^B_{\boldsymbol{R}+\boldsymbol{r}_\gamma-\boldsymbol{r}_z}\,|0^{\boldsymbol{R},\alpha}\rangle = -0.6689\,\mathrm{sgn}(K).$$

[1] A. Kitaev, Anyons in an exactly solved model and beyond, Ann. Phys. (NY) **321**, 2 (2006).

[2] L. Savary and L. Balents, Quantum spin liquids: A review, Rep. Prog. Phys. **80**, 016502 (2017).

[3] J. Knolle and R. Moessner, A field guide to spin liquids, Annu. Rev. Condens. Matter Phys. **10**, 451 (2019).

[4] G. Jackeli and G. Khaliullin, Mott insulators in the strong spin-orbit coupling limit: From Heisenberg to a quantum compass and kitaev models, Phys. Rev. Lett. **102**, 017205 (2009).

[5] S. Trebst and C. Hickey, Kitaev materials, Phys. Rep. **950**, 1 (2022).

[6] A. Banerjee, C. A. Bridges, J.-Q. Yan, A. A. Aczel, L. Li, M. B. Stone, G. E. Granroth, M. D. Lumsden, Y. Yiu, J. Knolle, S. Bhattacharjee, D. L. Kovrizhin, R. Moessner, D. A. Tennant, D. G. Mandrus, and S. E. Nagler, Proximate Kitaev quantum spin liquid behaviour in a honeycomb magnet, Nat. Mater. **15**, 733 (2016).

[7] Y. Wang, G. B. Osterhoudt, Y. Tian, P. Lampen-Kelley, A. Banerjee, T. Goldstein, J. Yan, J. Knolle, H. Ji, R. J. Cava, J. Nasu, Y. Motome, S. E. Nagler, D. Mandrus, and K. S. Burch, The range of non-Kitaev terms and fractional particles in $\alpha-\mathrm{RuCl_3}$, npj Quantum Mater. **5**, 14 (2020).

[8] R. D. Johnson, S. C. Williams, A. A. Haghighirad, J. Singleton, V. Zapf, P. Manuel, I. I. Mazin, Y. Li, H. O. Jeschke, R. Valenti, and R. Coldea, Monoclinic crystal structure of $\alpha-\mathrm{RuCl_3}$ and the zigzag antiferromagnetic ground state, Phys. Rev. B **92**, 235119 (2015).

[9] J. A. Sears, M. Songvilay, K. W. Plumb, J. P. Clancy, Y. Qiu, Y. Zhao, D. Parshall, and Y. J. Kim, Magnetic order in α-$\mathrm{RuCl_3}$: A honeycomb-lattice quantum magnet with strong spin-orbit coupling, Phys. Rev. B **91**, 144420 (2015).

[10] J. Chaloupka, G. Jackeli, and G. Khaliullin, Zigzag magnetic order in the iridium oxide Na_2IrO_3, Phys. Rev. Lett. **110**, 097204 (2013).

[11] M. Gohlke, R. Verresen, R. Moessner, and F. Pollmann, Dynamics of the Kitaev-Heisenberg model, Phys. Rev. Lett. **119**, 157203 (2017).

[12] J. Knolle, S. Bhattacharjee, and R. Moessner, Dynamics of a quantum spin liquid beyond integrability: The Kitaev-Heisenberg-Γ model in an augmented parton mean-field theory, Phys. Rev. B **97**, 134432 (2018).

[13] J. Wang, B. Normand, and Z.-X. Liu, One proximate Kitaev spin liquid in the K-J-Γ Model on the Honeycomb lattice, Phys. Rev. Lett. **123**, 197201 (2019).

[14] M. Gohlke, J. C. Pelayo, and T. Suzuki, Proximate tomonaga-luttinger liquid in an anisotropic Kitaev-Gamma model, Phys. Rev. B **109**, L220410 (2024).

[15] J. Chaloupka, G. Jackeli, and G. Khaliullin, Kitaev-Heisenberg model on a honeycomb lattice: possible exotic phases in iridium oxides A_2IrO_3, Phys. Rev. Lett. **105**, 027204 (2010).

[16] S.-S. Zhang, G. B. Halász, W. Zhu, and C. D. Batista, Variational study of the Kitaev-Heisenberg-Gamma model, Phys. Rev. B **104**, 014411 (2021).

[17] S.-S. Zhang, G. B. Halasz, and C. D. Batista, Theory of the kitaev model in a [111] magnetic field, Nat. Commun. **13**, 399 (2022).

[18] C. Chen and I. S. Villadiego, Nature of visons in the perturbed ferromagnetic and antiferromagnetic Kitaev honeycomb models, Phys. Rev. B **107**, 045114 (2023).

[19] A. P. Joy and A. Rosch, Dynamics of visons and thermal Hall effect in perturbed Kitaev models, Phys. Rev. X **12**, 041004 (2022).

[20] A. P. Joy and A. Rosch, Gauge field dynamics in multilayer Kitaev spin liquids, npj Quantum Mater. **9**, 62 (2024).

[21] K. B. Yogendra, T. Das, and G. Baskaran, Emergent glassiness in the disorder-free Kitaev model: Density matrix renormalization group study on a one-dimensional ladder setting, Phys. Rev. B **108**, 165118 (2023).

[22] E. H. Lieb, Flux phase of the half-filled band, Phys. Rev. Lett. **73**, 2158 (1994).

[23] J.-P. Blaizot and G. Ripka, *Quantum Theory of Finite Systems* (MIT Press, Cambridge, 1986).

[24] A. Panigrahi, P. Coleman, and A. Tsvelik, Analytic calculation of the vison gap in the Kitaev spin liquid, Phys. Rev. B **108**, 045151 (2023).

[25] F. Zschocke and M. Vojta, Physical states and finite-size effects in Kitaev's honeycomb model: Bond disorder, spin excitations, and NMR line shape, Phys. Rev. B **92**, 014403 (2015).

[26] T. Grace, Variational construction of ground state of Kitaev spin liquid with vison pair supporting julia code (2025), available at: https://doi.org/10.48420/30752867.